Precise half-life measurements for the superallowed β^+ emitters ^{34}Ar and ^{34}Cl

V. E. Iacob,* J. C. Hardy, J. F. Brinkley, C. A. Gagliardi, V. E. Mayes, N. Nica, M. Sanchez-Vega, G. Tabacaru, L. Trache, and R. E. Tribble

Cyclotron Institute at Texas A&M University, College Station, Texas 77843-3366, USA

(Received 8 August 2006; published 28 November 2006)

To contribute meaningfully to any test of the unitarity of the Cabibbo-Kobayashi-Maskawa (CKM) matrix, the measured *ft* value of a superallowed $0^+ \rightarrow 0^+$ β^+ transition must be obtained to a precision of 0.1% or better. We have determined the half-life of the superallowed emitter ^{34}Ar to be 843.8(4)ms; the quoted precision, 0.05%, is a factor of five improvement on the best previous measurement and meets this demanding requirement. Our measurement employed a high-efficiency gas counter, which was sensitive to positrons from both ^{34}Ar and its daughter ^{34}Cl. We achieved the required precision on ^{34}Ar by analyzing the parent-daughter composite decay with a new fitting technique. We also obtained an improved half-life for ^{34}Cl of 1.5268(5) s, which has 0.03% precision and is a factor of two improvement on previous results. As a by-product of these measurements, we determined the half-life of ^{35}Ar to be 1.7754(11) s.

DOI: 10.1103/PhysRevC.74.055502 PACS number(s): 21.10.Tg, 23.40.−s, 27.30.+t

I. INTRODUCTION

The unitarity of the Cabibbo-Kobayashi-Maskawa (CKM) matrix is a fundamental requirement of the three-generation Standard Model. Currently, the most demanding test available of CKM unitarity is the sum of squares of the experimentally determined elements of the matrix's top row [1]. The dominant term in this test is the up-down quark-mixing element, V_{ud}, the most precise value of which is obtained through nuclear measurements of superallowed $0^+ \rightarrow 0^+$ beta decays. To date, the measured *ft* values for transitions from nine different nuclei are known to ~0.1% precision and four more to $\leqslant 0.5\%$ [1,2]. So far, the superallowed transition from ^{34}Ar has been in the latter category, its *ft*-value precision being 0.5%.

In principle, the precise *ft* value for a single superallowed $0^+ \rightarrow 0^+$ transition would be sufficient to determine V_{ud}, but if 0.1% precision or better is the goal, the uncertainties associated with the calculated correction terms that must be applied to the data would become a serious obstacle. The measured *ft* value relates to the vector coupling constant, $G_{\rm v}$ – and, through it, to V_{ud} – via the relationship [1]

$$\mathcal{F}t \equiv ft(1+\delta'_R)(1+\delta_{NS}-\delta_C) = \frac{K}{2G_{\rm v}^2\left(1+\Delta_{\rm R}^{\rm v}\right)}, \qquad (1)$$

where $K/(\hbar c)^6 = 2\pi^3\hbar \ln 2/(m_e c^2)^5 = 8120.271(12) \times 10^{-10}$ GeV^{-4}s, δ_C is the isospin-symmetry-breaking correction and $\Delta_{\rm R}^{\rm v}$ is the transition-independent part of the radiative correction. The terms δ'_R and δ_{NS} comprise the transition-dependent part of the radiative correction, the former being a function only of the electron's energy and the Z of the daughter nucleus, while the latter, like δ_C, depends in its evaluation on the details of nuclear structure. Both δ_C and δ_{NS} have been calculated [3] with the best available shell-model wave functions, which are based on a wide range of spectroscopic data. They were further tuned to agree with measured binding energies, charge radii and coefficients of the isobaric multiplet mass equation. Even so, if only a single precise *ft* value were known, the validity of these structure-dependent corrections would be without independent verification, and the derived value for $G_{\rm v}$ could be in doubt.

What has given credibility to the nuclear result for $G_{\rm v}$ is the fact that many superallowed transitions have been measured precisely and all give statistically identical results for $\mathcal{F}t$ – and hence for $G_{\rm v}$. Since the uncorrected *ft* values actually scatter over a relatively wide range, it is the structure-dependent corrections that are responsible for bringing the $\mathcal{F}t$ values into agreement with one another. Obviously, this is already a powerful experimental validation of the calculated corrections themselves, but it can still be improved further by precise measurements of additional transitions, ones calculated to have large correction terms. If the *ft* values measured for cases with large calculated corrections also turn into corrected $\mathcal{F}t$ values that are consistent with the others, then this reinforces the calculations' reliability for cases where the corrections are smaller. The superallowed transition from ^{34}Ar is one of those cases with relatively large calculated correction terms: $\delta_C - \delta_{NS} = 0.83(4)\%$ [3].

The *ft* value that characterizes any β-transition depends on three measured quantities: the total transition energy, Q_{EC}, the half-life, $t_{1/2}$, of the parent state, and the branching ratio, R, for the particular transition of interest. The Q_{EC}-value is required to determine the statistical rate function, f, while the half-life and branching ratio combine to yield the partial half-life, t. The Q_{EC} value for ^{34}Ar is already known sufficiently well [4] to yield a value for f with 0.04% precision [1] but, before the measurement reported here, the ^{34}Ar half life was only known to 0.4% and its branching ratio to 0.3% [5]. Our half-life for ^{34}Ar has 0.05% precision and represents the first step in bringing the *ft* value for this transition into the desired range of 0.1%. The second step will be an improved branching ratio, a measurement that is currently nearing completion.

A byproduct of our ^{34}Ar half-life measurement was an improved result for the half-life of its daughter ^{34}Cl, which is

*Email address: iacob@comp.tamu.edu

another superallowed emitter. Both results replace preliminary values reported in Ref. [6].

II. THE EXPERIMENTAL SET-UP

Precise half-life measurements need high-purity radioactive beams, a requirement that is even more important for cases where the daughter nucleus is itself radioactive. We achieved this goal by using production reactions with inverse kinematics, and selecting the desired reaction products with the Momentum Achromat Recoil Separator (MARS) [7]. Primary beams of ^{35}Cl at 25 and 30A MeV produced by the superconducting cyclotron at Texas A&M University impinged on a 1.6-atm hydrogen gas target cooled to liquid nitrogen temperature. The fully stripped ejectiles were then analyzed by MARS. Initially, working with a low-current primary beam, we inserted at the focal plane of MARS a 5×5 cm silicon telescope consisting of a 16-strip position-sensitive detector (PSD) 300 μm thick, backed by a 1-mm-thick detector. The telescope was used first for the identification of secondary reaction products, then for the control of the selection and focus of the desired species in the center of the beam line. This also gave us a clear indication of nearby reaction products that could potentially contribute to our selected beam.

After the tuning and selection procedure, the PSD detector was dropped out of the way and the intensity of the primary beam was increased. With extraction slits at the MARS focal plane used to select a particular reaction product, the resulting radioactive beam was extracted into air through a 51-μm-thick kapton window. This beam passed through a 0.3-mm thin BC-404 plastic scintillator and through a set of aluminum degraders, eventually being implanted in the 76-μm-thick aluminized mylar tape of a fast tape-transport system. The scintillator allowed us to count the implanted nuclei, while the degraders ensured that they were implanted in the middle of the tape. The combination of m/q selectivity in MARS and range selectivity in the degraders led to implanted samples that were substantially better than 99% pure.

After the radioactive sample had been collected for a time interval of the order of one half-life, the beam was turned off and the tape-transport system moved the sample 90 cm to a well-shielded location in less than 0.2 s, stopping it in the center of a 4π proportional gas counter, which is constructed in two halves with a very narrow slot between to accommodate the tape. The performance of this type of detector is well known [8–10]. When operated in the proportional region, as ours is, all but a small fraction ($\ll$1%) of the amplified signals exceed the discriminator threshold, thus rendering the counter essentially 100% efficient for charged-particle radiation. The signals from the discriminator were then multiscaled for up to 20 half-lives, and a 500-channel time spectrum recorded. Such collect-move-detect cycles were repeated, with a separate decay spectrum recorded for each, until the desired overall statistics had been achieved. In its shielded location, the gas counter had a background count rate of about 0.5 counts/s, which was 3–4 orders of magnitude lower than the initial count rate for each collected sample.

The electronic chain involved in the measurement is presented in Fig. 1. It comprises the detector, which was powered

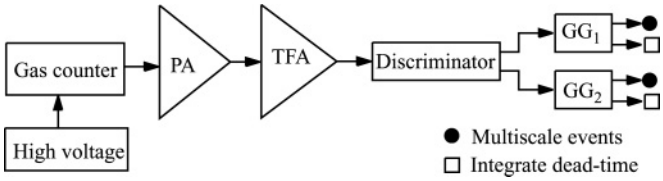

FIG. 1. Electronic chain. Gas-counter signals are amplified by a preamplifier (PA) and a timing-filter amplifier (TFA); then go to a low-level discriminator, whose output is sent to two gate generators (GG), each of which introduces a well defined, but different, dead time. Finally, the gate-generator signals are multiscaled and their width is monitored.

by a high voltage supply; a preamplifier (Phillips Scientific, model 6950); a Timing Filter Amplifier (Ortec, model 579); a discrimintor (Phillilps Scientific, model 711); two fixed-width nonretriggering and nonextending gate generators (Phillips Scientific, model 794); and two CAMAC multichannel scalers (Data Design Corporation, model IS10A). To ensure the desired precision, the time base for the acquired spectra was defined by a Stanford Research System pulser (Synthesized Function Generator, model DS345), which is accurate to 0.01 ppm. The gate generators in the electronic scheme introduced fixed and well known dead times, which were selected to be longer than any other up-stream dead-time contributions. We set the widths of these gates (dead times) to be different from one another, and frequently changed them from run to run. Both gates also were continuously monitored during every run, thus giving us an on-line measure of the dead-time correction during data collection. Note that even though the two gate generators were fed by the same data, the dead-time distortions of the underlying Poisson-distributed data are independent in the two cases; thus the two data streams allowed us to test that our dead-time corrected result was independent of the actual dead time of the circuit.

We also tested thoroughly for systematic effects caused by other adjustable detection parameters. Every experiment was subdivided into many separate runs, differing only in their detection parameters: dominant dead-time, detector bias and discrimination threshold. Since our detector is very nearly 100% efficient, one would not expect our results to be sensitive to changes in the discriminator threshold or the detector bias (so long as the detector continued to operate in the proportional region). Nevertheless, we separately analyzed the individual runs to test for such effects and also to allow us to assess the uncertainty on the final result. No systematic trends were identified with any of these parameters.

As the measurements were aimed at better than 0.1% precision, other special precautions were taken too. For example, the tape-transport system is quite consistent in placing the collected source within ±3 mm of the center of the detector, but it is a mechanical device, and occasionally larger deviations occur. Although there is no reason to expect that this could lead to a false half-life result, we separately recorded the number of implanted nuclei detected in the scintillator at the beginning of each cycle, and the number of positrons recorded in the gas counter during the subsequent count period. The ratio of the latter to the former is a sensitive measure of whether the

source is seriously misplaced in the proportional counter. In analyzing the data later, we rejected the results from any cycle with an anomalous (low) ratio. This happened rarely: less than 0.3% of the cycles were rejected.

III. RESULTS

The measurement of the ^{34}Ar half-life faced two special challenges:

(i) ^{34}Ar is a noble gas and this raises the possibility that some of the implanted atoms might diffuse out of the mylar tape during the counting time interval. If this were to occur, it would reduce the amount of activity present in the tape (but not necessarily in the sensitive region of the detector) as a function of time, possibly simulating a half-life shorter than the real one. We address this problem in Sec. III A.

(ii) The daughter nucleus ^{34}Cl is radioactive with a half life comparable to that of ^{34}Ar. Since our gas counter cannot discriminate between the two activities, we obtain a composite decay curve. Under these conditions, if the daughter half-life were exactly a factor of two greater than the parent one, the decay curve would be a single exponential function exhibiting the half-life of the daughter! In our case, the ^{34}Cl half-life is actually 1.8 times that of ^{34}Ar, but this is close enough to two that special techniques (and an additional experiment) had to be employed to extract a precise half-life for ^{34}Ar from our data. These will be detailed in Secs. III B and III C.

To address these challenges, two supplementary experiments were performed. In the first, we measured the decay of ^{35}Ar. This nuclide has a well known half-life, which is comparable to that of ^{34}Ar. If there were any significant diffusion of the noble-gas atoms during our detection time, its effects would appear in our measured half-life for ^{35}Ar. In the second experiment, we measured the half-life of ^{34}Cl in order to improve its accuracy. An important requirement for extracting the parent half-life from a composite parent-daughter decay curve is that the half-life of the daughter nucleus be well known. Otherwise its uncertainty would dominate the error budget in the result for the parent half-life.

A. The ^{35}Ar experiment

The currently accepted value for the half-life of ^{35}Ar, 1.775(4) s [11], is the average of four concordant measurements, the two most precise being 1.774(3) s [12] and 1.770(6) s [13]. Quite different techniques from ours were used in these measurements: ^{35}Ar was produced by (p, n) reactions in targets of LiCl, CCl_4, KCl, and $PbCl_2$ at proton beam energies between 7 and 13 MeV; the activity remained in the target, where it was counted. In one case [12], the LiCl target was encapsulated in a berylium cylinder; in another [13], the diffusion issue was specifically addressed, with several different targets and configurations being tested, including a KCL target covered with a tantalum foil to inhibit diffusion.

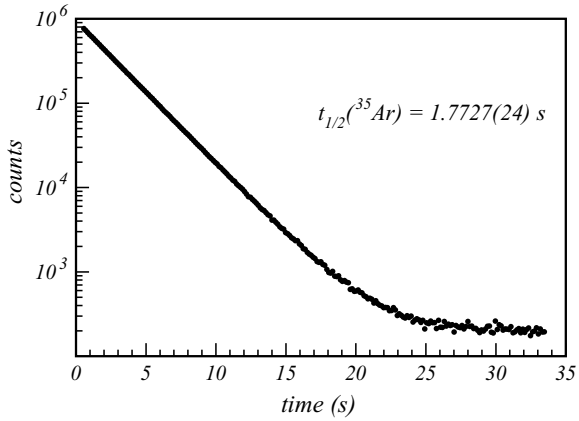

FIG. 2. Total time-spectrum recorded for the β^+ decay of ^{35}Ar.

No evidence for diffusion losses was found in those tests, and the agreement among the diverse measurements from four different experimental teams further testifies to the absence of such losses in any of them since it would be hard to imagine that diffusion losses, if they existed, would be identical for them all. Thus, we can consider that 1.775(4) s is a valid half-life value for ^{35}Ar in the absence of diffusion losses.

In our experiment, we produced ^{35}Ar via the reaction $p(^{35}\mathrm{Cl}, n)^{35}\mathrm{Ar}$ at a bombarding energy of 25A MeV. The ^{35}Ar recoils were separated in MARS, counted, degraded and implanted in tape. The half-life of ^{35}Ar was measured under the same conditions used for our main ^{34}Ar experiment except that the counting period was 35 s, nearly three times longer than we used for the latter measurement. The decay spectrum is presented in Fig. 2: it represents a total of 16×10^6 events recorded in about 2800 cycles. From these data, we obtained a half-life of $t_{1/2}(^{35}\mathrm{Ar}) = 1.7754(11)$ s.

The uncertainty on the known half-life of ^{35}Ar is 0.2% and our result, which is actually even more precise than that, is in excellent agreement with it. Consequently, we may conclude that there is no experimental evidence of diffusion effects in our experiment over a 35-s period, and that we may now be confident that any possible effects are completely negligible for the 12-s period that we used to study ^{34}Ar.

This conclusion is further supported by simple diffusion calculations. The diffusivity of argon in a biaxially oriented polyester (Mylar is a trade name for such a material) is measured to be in the range of 5×10^{-10} cm^2/s [14]. Taking account of the measured distribution of activity deposited in our tape, we calculate that no more than 0.002% of implanted ^{34}Ar atoms could leave the tape during the 12 s counting period. This is already a negligible effect, even at our precision, but it is made still more so by consideration of what would happen to any atom that did diffuse out of the tape. Such atoms would find themselves in the narrow air gap between the halves of the proportional counter, where their decays would still be detected just as if they had decayed while in the tape. We can then ask how far these atoms might diffuse in air during our counting period. Kinetic theory of gases, in a hard-sphere model for molecules, can be used to give an estimate for the distance that an Ar atom diffuses in air as a function of time. Taking molecular diameters from viscosity

measurements [15], we calculate the mean free path for an Ar atom drifting at room temperature in air to be 7.1×10^{-8} m, which corresponds to a diffusion distance of 1.1 cm in 12 s. This estimated distance is well within the 1.8-cm sensitive detector region and any decay occurring within that time period from a diffusing atom would be detected with the same ~100% efficiency as one that occured from an atom in the tape. Clearly, diffusion from the tape need not be a concern in our measurement.

B. The ^{34}Cl experiment

We produced ^{34}Cl by bombarding the cooled hydrogen target with a 25A-MeV ^{35}Cl beam to initiate the $p(^{35}\mathrm{Cl}, pn)^{34}\mathrm{Cl}$ reaction. A high-purity beam of fully stripped ^{34}Cl ions with 20A MeV was extracted from the focal plane of the MARS spectrometer. After passing through the window, scintillator and degraders, these ions were implanted in the tape of our tape-transport system. The collected sample consisted of two components: the 0^+ ground-state of ^{34}Cl ($t_{1/2} = 1.53$ s) and the 3^+ isomeric state of ^{34}Cl ($t_{1/2} = 32.2$ min). In principle, the beam extracted from MARS might also have contained a very small amount of ^{30}P ($t_{1/2} = 150$ s), which has the same m/q ratio as ^{34}Cl, but the range of ^{30}P is different from that of ^{34}Cl so the amount stopping in the tape would be even smaller. We checked for this possibility, however, by making separate measurements with two different sets of aluminum degraders, each chosen to increase the amount of ^{30}P stopped in the tape if, indeed, any were present in the separated beam. No indication of ^{30}P was found.

In this experiment, the collect/move/detect time intervals were 3 s/0.18 s/35 s but, unlike most of the other measurements reported here, for technical reasons only a single dead-time chain at a time was used (cf. Fig. 1). The decay curve for the sum of all accepted cycles is presented in Fig. 3: it represents a total of about 24×10^6 ^{34}Cl decays recorded over a time equal to 23 of its half-lives. As a means of uncovering any possible systematic errors, the experiment was divided into 27 separate runs, each with different settings of the adjustable detection parameters. Various combinations of dominant dead-times (10 or 12μs), detector bias (2600, 2700, and 2800 V) and discrimination threshold (150 or

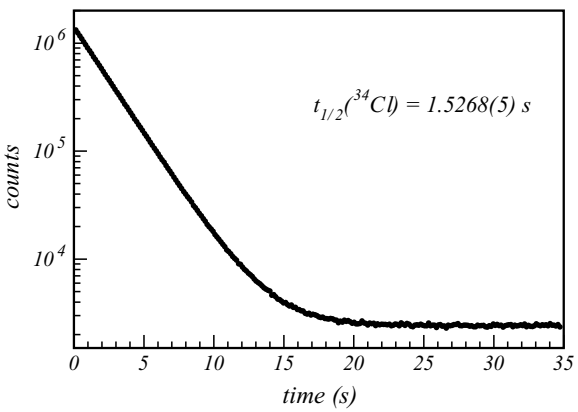

FIG. 3. Total time-decay spectrum recorded for the β^+ decay of ^{34}Cl.

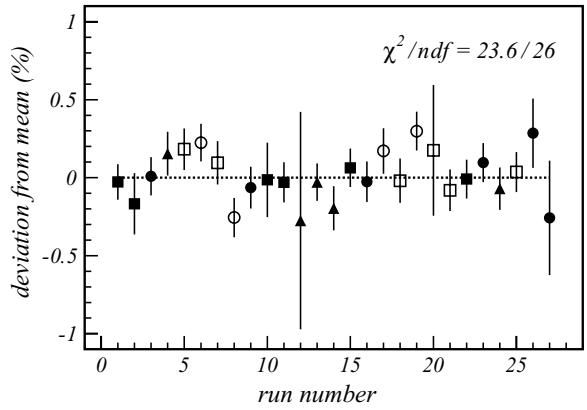

FIG. 4. Test for possible systematic bias in the ^{34}Cl half-life measurement due to the discriminator threshold or detector bias. Full/open symbols represent the two 150 mV/200 mV discriminator settings; circles/squares/triangles represent, respectively, the detection biases 2600 V/2700 V/2800 V.

200 mV) were used. We then individually analyzed the data from each run with a maximum-likelihood fit to the spectrum obtained by our summing the dead-time-corrected spectra from all accepted cycles. No indication of a systematic bias was evident when these measurements were compared. Figure 4 shows the results from each run with the detector bias and discriminator setting of each indicated. The results, which are already dead-time corrected, were equally insensitive to the actual circuit dead-time used in each run.

As a further systematic check, in this case on the fitting procedure, we generated by Monte Carlo techniques a set of spectra which matched, cycle by cycle, the statistics and composition of the data from each cycle. The half-life we used in generating these spectra was chosen to be similar to that of ^{34}Cl. We then fitted these artificial data with the same techniques we used for the real data. The half-life we obtained from fitting our artificial data agreed with the input half-life within statistical uncertainties, thus validating the fitting procedure and the result obtained from it.

We also checked for the possible presence of short-lived impurities or other possible count-rate dependent effects. We removed data from the first 1.4 s of the counting period in each measurement and refitted the remainder; then we repeated the procedure, removing the first 2.8 s, 4.2 s, and so on. As can be seen from Fig. 5, within statistics the derived half-life was also stable against these changes.

Our result, $t_{1/2}(^{34}\mathrm{Cl}) = 1.5268(5)$ s, is consistent with the most precise previous results cited in a recent survey [1] of world data, 1.5260(20) s [16], 1.5252(11) s [17], and 1.5277(22) s [9] but its precision is more than a factor of two better than any of them.

C. The ^{34}Ar experiments

A high-purity beam of ^{34}Ar was produced via the $p(^{35}\mathrm{Cl}, 2n)^{34}\mathrm{Ar}$ reaction at a ^{35}Cl bombarding energy of 30A MeV. As in our other experiments, the ^{34}Ar ions separated in MARS were stopped in tape after passing through the

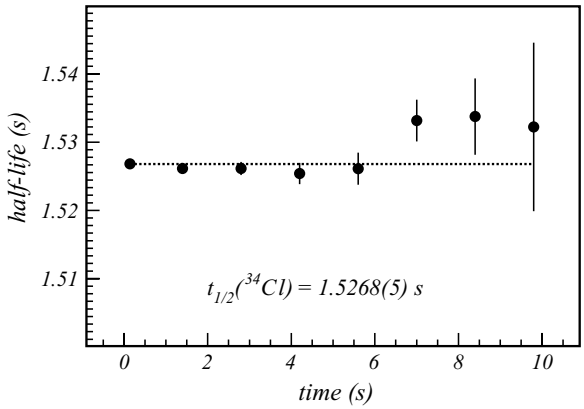

FIG. 5. Test for possible systematic errors in the measurement of the decay of ^{34}Cl caused by undetected short-lived impurities or by rate-dependent counting losses. The abscissa represents the time period at the beginning of the counting cycle for which the data were omitted from the fit.

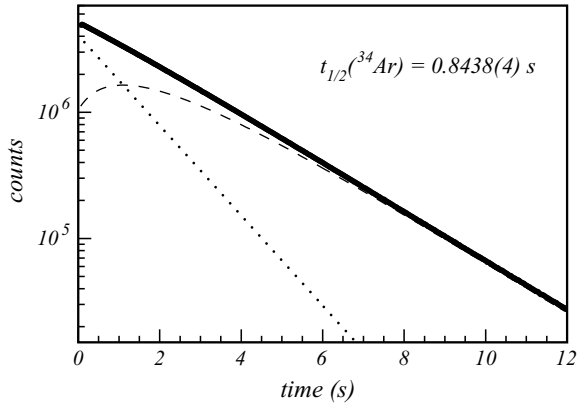

FIG. 6. Total time-decay spectrum obtained for the β^+ decay of ^{34}Ar and its daughter ^{34}Cl. The dotted/dashed lines represent the calculated ^{34}Ar/^{34}Cl contributions.

Kapton window, a plastic scintillator and a stack of aluminum degraders. Each ^{34}Ar sample was collected for either 0.7 or 1 s, and then moved in 0.18 s to the center of the 4π proportional gas counter. Signals from the counter were multiscaled for a period of 12 s.

We collected a total of about 400×10^6 decay events in two separate experiments. The first one included about 180×10^6 events from 20,800 tape cycles, which were split into 40 separate runs. In this case, only one dead-time chain was used, but dead-times of 10 and 12 μs were used alternately in successive runs. In the second experiment, both dead-time chains operated and another 220×10^6 events were collected in 14,700 cycles split into 24 separate runs. For both experiments, each run was characterized by different settings of the adjustable detection parameters. The various combinations included dead-times of 3, 4, 6, 8, 10, and 12 μs; detector biases of 2400, 2550, and 2700 V; and discrimination thresholds of 150 and 200 mV. The main difference between the two experiments was the purity of the beam in the focal plane of MARS: the only significant impurity, ^{33}Cl ($t_{1/2} = 2.51$ s)—as identified in the PSD at the MARS focal plane—was at a level of 0.3% relative to ^{34}Ar in the first experiment, but increased to 0.7% in the second.

Though small in both experiments, the ^{33}Cl impurity was of enough concern that we dedicated several runs to investigating how much of this activity actually survived the range-purification of the degrader, and appeared in our collected samples. In one of these runs, we collected activity for 5 s and counted for 50 s; in the other, we collected for 20 s and counted for 60 s. These times were chosen to enhance the effects of the longer-lived impurity on the decay spectra. We determined from the analysis of these spectra that the degrader decreased the ^{33}Cl impurity in the collected samples by a factor of 3 relative to ^{34}Ar, and that in the first experiment described in the last paragraph we had 0.1% ^{33}Cl in the collected samples and in the second, 0.2%. We conservatively assigned 100% uncertainties (i.e., $\pm 0.1\%$ and $\pm 0.2\%$, respectively) to these two results and used them in the subsequent analysis of all our ^{34}Ar data.

We processed the data run-by-run by summing the dead-time-corrected spectra from all the cycles included in each run. The total time-decay spectrum obtained from the combined experiments is presented in Fig. 6, where we also show the separate contributions from the ^{34}Ar parent and ^{34}Cl daughter. This breakdown into components comes from a calculation based upon our final analysis and is presented here simply to illustrate the problems we faced in analyzing the data. Clearly the decay of ^{34}Ar is almost completely masked by the growth of its daughter. The experimental decay curve only differs very slightly from a single exponential with the daughter's half-life.

We can easily understand this situation by examining the coupled decay equations for combined parent-daughter decays. The combined ^{34}Ar and ^{34}Cl activity is given by

$$\Lambda_{\text{tot}} = C_1 e^{-\lambda_1 t} + C_2 e^{-\lambda_2 t}, \tag{2}$$

where

$$C_1 = N_1 \lambda_1 \frac{2\lambda_2 - \lambda_1}{\lambda_2 - \lambda_1}, \qquad C_2 = N_2 - \frac{N_1 \lambda_1}{\lambda_2 - \lambda_1}, \tag{3}$$

where t is the time elapsed after the end of the collect period, $N_{1,2}$ are the numbers of ^{34}Ar and ^{34}Cl nuclei present in the source at $t = 0$, and $\lambda_{1,2}$ are the corresponding decay constants. Note that when $\lambda_1 = 2\lambda_2$ the coefficient C_1 vanishes, leaving a single exponential term having the decay constant of ^{34}Cl. Although not related exactly by a factor of 2, the actual half-lives of ^{34}Ar and ^{34}Cl are close enough that, for our measurements, the coefficient C_1 was more than six times smaller than the coefficient C_2, and was negative. This is a serious limitation for any conventional two-component fit of the data. Even with the more than 400×10^6 events in our data, our initial analysis yielded the value 847.0(37) ms for the half-life of ^{34}Ar, a result with only 0.4% precision. We reported this value as a preliminary result several years ago [6].

Unsatisfied with this relatively imprecise result, we performed a new experiment in which we introduced thin copper foils as degraders between the source on the tape and each half of the gas counter. Since the end-point energy of the

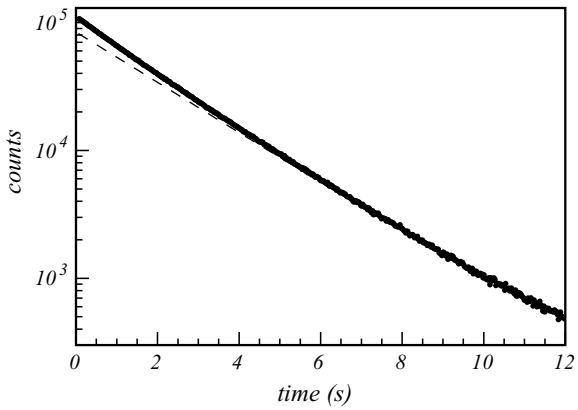

FIG. 7. Total time-decay spectrum obtained for the β^+ decay of ^{34}Ar with copper degraders around the source to preferentially reduce the ^{34}Cl contribution. There were more than 9×10^6 combined ^{34}Ar and ^{34}Cl events. The dashed line shows the contribution of the exponential with the ^{34}Cl decay constant.

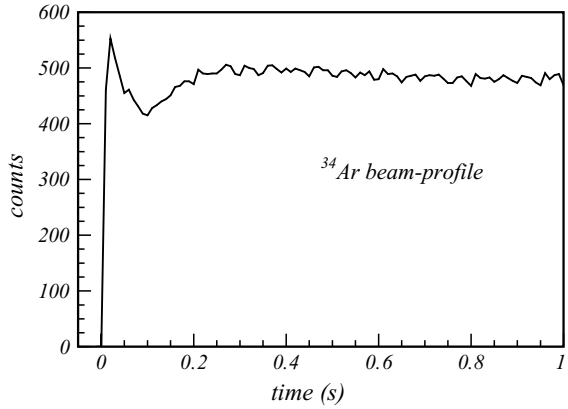

FIG. 8. Typical time-profile of the collected ^{34}Ar beam. The initial drop in intensity is generated by the lowering of the gas density as the primary beam heats the gas around its path. A fan located inside the gas-target speeds up the transition to stable conditions.

β^+ spectrum of ^{34}Cl (4.47 MeV) is lower than that of ^{34}Ar (5.04 MeV), we sought to preferentially attenuate positrons from the former, thus increasing the contribution of the latter to the composite spectrum. The total decay-spectrum produced in this experiment appears in Fig. 7. Obviously, the contribution from the exponential with the ^{34}Ar decay constant is more prominent and is no longer negative but, after we had successfully optimized the thickness of copper degraders to improve the C_1/C_2 ratio from 1/6 (negative) to about 3 (positive), we had paid a high price: our count-rate had been cut to 5% of the unattenuated rate. With a total of 9.5×10^6 combined ^{34}Ar and ^{34}Cl decay events recorded under this optimal condition, we obtained an ^{34}Ar half-life of 844.4(47) ms, a result with 0.6% precision, which was worse than before. Even though the improved decay spectra had made the ^{34}Ar contribution more prominent, this advantage was more than offset by our loss in counting statistics.

Having failed to find an experimental solution we returned to our original data seeking an improved method of analysis. A close look at Eqs. (2) and (3) revealed that the near cancellation of the C_1 coefficient could actually be turned to our advantage: instead of solving for the two components independently, we could focus on the difference between the experimental data and a one-component decay, and use that difference to determine the amount by which the ratio of the two half-lives deviates from 2. However, for this type of analysis to be effective, we needed an independent determination of the value of N_2/N_1 from our experiment.

If the ^{34}Ar-sample collection rate had been constant, this ratio could have been determined from a simple calculation of the production of ^{34}Cl (via ^{34}Ar decay) over the collection period. Unfortunately, although the collection rate was very nearly constant over most of the collection period, it was evident from the measured rate in the scintillator at the exit of MARS, which detected the separated ^{34}Ar ions as a function of time, that there were noticeable variations at the beginning of the collection period (see Fig. 8). Our cryotarget is a gas, and the primary beam heats that gas around its path through the target, thus initially generating a local drop in gas density; the transition to steady conditions, which are observed after 0.2 s, is hastened by a fan that continuously circulates the gas in the target cell, but those initial fluctuations are sufficient to affect the ratio N_2/N_1. We also found that the amplitude of the drop in the radioactive beam intensity depended on the primary beam intensity, slightly changing the beam-profile from one cycle to another. With the collection profile measured, however, we could perform numerical integrations over the measured ^{34}Ar accumulation and the calculated decay-production of ^{34}Cl during the collection period in order to obtain the N_2/N_1 ratio for each cycle.

With this approach, the fitting procedure becomes more computer intensive but the reward is its effectiveness in increasing the precision of the extracted half-life. To test our new approach and its improved statistical precision, we

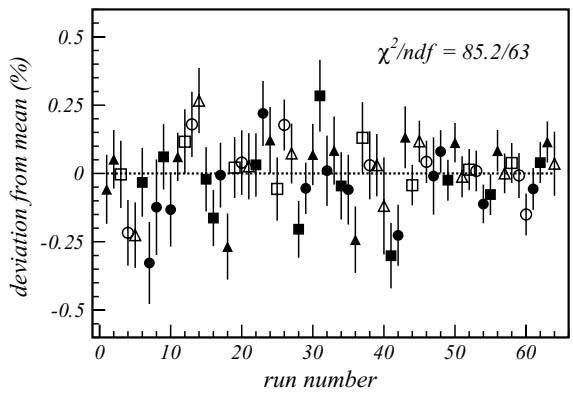

FIG. 9. Test for possible systematic bias in the ^{34}Ar half-life measurement due to discriminator threshold or detector bias. Full/open symbols represent the two 150 mV/200 mV discriminator settings; circles/squares/triangles represent respectively the detection biases 2400 V/2550 V/2700 V. The result from each run is compared to the average value for the experiment to which it belongs. Runs 1–40 comprise the first experiment, contain a total of about 180×10^6 events, and have $\chi^2/ndf = 54.6/39$; while runs 41–64 comprise the second experiment, contain about 220×10^6 events, and have $\chi^2/ndf = 30.6/23$.

TABLE I. Error budget for the two ^{34}Ar experiments: experiment no. 1 contained 180×10^6 events and experiment no. 2 contained 220×10^6 events.

Source	Error (ms)	
	Experiment no. 1	Experiment no. 2
statistics	0.19	0.16
^{33}Cl impurity	0.27	0.48
$t_{1/2}(^{34}\mathrm{Cl})$	0.13	0.13
dead-time	0.10	0.15
tape transit time	0.10	0.10
^{34}Cl impurity	0.07	0.11
beam time-profile	0.05	0.05
bias/threshold	0.04	0.04
half-life (ms)	843.54(39)	844.38(57)

generated a parallel set of artificial spectra by Monte Carlo techniques: these spectra mimicked our experimental data in statistics, background, dead-time and sample-collection profile, but with an imposed half-life of 845 ms for the parent activity. The results we obtained in fitting this pseudo-data were statistically consistent with the half-life used in generating them. This demonstrated the reliability of our new fitting procedure.

In our analysis of the experimental data themselves, we also tested for the stability of the fitted half-life as a function of various detection settings. As seen in Fig. 9, the half-life results show no systematic dependence on detector bias or discriminator threshold. Although not illustrated, our results were also found to be independent of the circuit dead time in both experiments. The results from the two experiments also agreed reasonably well with one another (see Table I). Our final result thus represents a self-consistent analysis of more than 400×10^6 combined ^{34}Ar and ^{34}Cl decay events. We determine the final half-life to be $t_{1/2}(^{34}\mathrm{Ar}) = 843.8(4)$ ms, a result that is consistent with, but significantly more precise than, the only comparable previous result for the ^{34}Ar half-life, 844.5(34) [5].

Our quoted uncertainty contains contributions from a variety of sources, as itemized in Table I. Counting statistics were not the largest contributor to the uncertainty in either experiment. Earlier in this section we discussed the presence of a small (0.1–0.2%) ^{33}Cl impurity in our samples, and it was the effects of this impurity that dominated the uncertainties in both experiments. The next most significant contributors were the uncertainties from the measured half-life of ^{34}Cl, from the dead-time correction and from variations in the time taken to transfer each source from the collection point to the gas counter. At a somewhat lower level was the uncertainty associated with the possible direct production of ^{34}Cl; we could set a limit on directly produced ^{34}Cl from the PSD in the MARS focal plane and this value was used in determining its contribution to the overall uncertainty. Still smaller uncertainty contributions came from the time-profile of the beam and the scatter associated with different detector biases and discriminator thresholds.

IV. CONCLUSIONS

We report here the first measurement of the half-life of the superallowed β^+ emitter ^{34}Ar obtained with a precision better than 0.1%. This measurement required us to perform four separate experiments. In the first, by measuring the half life of ^{35}Ar, we determined that any possible diffusion of argon from our tape-implanted source did not occur on the time scale of our measurement. In the second, we measured the half-life of the superallowed emitter ^{34}Cl – the daughter of ^{34}Ar – with improved precision, an important step in increasing the accuracy with which we could determine the half-life of ^{34}Ar from the combined decay spectrum. In the last two experiments, we measured positrons from the combined ^{34}Ar and ^{34}Cl parent-daughter linked decays under different source conditions, acquiring more than 400 million events in all.

Because of the particular relationship between the ^{34}Ar and ^{34}Cl half-lives, we had to develop a special technique to analyze their combined decay spectrum, which required a precise knowledge of the rate of deposition of the ^{34}Ar source. The computer-fitting method then focused on the deviation of the observed time-decay spectrum from a single-component decay with the ^{34}Cl half-life. Possible sources of error were carefully investigated and an error budget established; the major contributor to the overall uncertainty was the very weak source contamination with ^{33}Cl.

Our new precise result for the ^{34}Ar half-life agrees well with the only previous measurement of comparable precision [5]. It should also be noted that this previous measurement used a different technique, which depended on the decay of the β-delayed γ-rays from the daughter ^{34}Cl. It is encouraging that the two results are in good agreement.

Finally, we remark that once the branching ratio for the superallowed transition from ^{34}Ar has been measured to comparable precision, the $\mathcal{F}t$ value for the transition will be known to a precision of $\sim$0.1%. It will then be in the same category as the best known superallowed transitions, but will have the largest calculated structure-dependent corrections of any of them. This will make it a particularly valuable case for testing the validity of these corrections. The branching-ratio measurement is currently in progress at our laboratory.

ACKNOWLEDGMENTS

This work was supported by the U.S. Department of Energy under Grant No. DE-FG03-93ER40773 and by the Robert A. Welch Foundation under Grant No. A-1397.

[1] J. C. Hardy and I. S. Towner, Phys. Rev. C **71**, 055501 (2005); Phys. Rev. Lett. **94**, 092502 (2005).
[2] T. Eronen *et al.*, Phys. Lett. **B636**, 191 (2006).
[3] I. S. Towner and J. C. Hardy, Phys. Rev. C **66**, 035501 (2002).
[4] F. Herfurth *et al.*, Eur. Phys. J. A **15**, 17 (2002).
[5] J. C. Hardy *et al.*, Nucl. Phys. **A223**, 157 (1974).

[6] V. E. Iacob, E. Mayes, J. C. Hardy, R. G. Neilson, M. Sanchez-Vega, A. Azhari, C. A. Gagliardi, L. Trache, and R. E. Tribble, Bul. Am. Phys. Soc. **48**, No. 2, 34 (2003).
[7] R. E. Tribble *et al*., Nucl. Phys. **A701**, 278 (2002).
[8] *A Handbook of Radioactivity Measurements Procedures*, National Council on Radiation Protection and Measurements report NCRP No. 58 (1978); see especially section 3.5.
[9] V. T. Koslowsky, E. Hagberg, J. C. Hardy, R. E. Azuma, E. T. H. Clifford, H. C. Evans, H. Schmeing, U. J. Schrewe, and K. S. Sharma, Nucl. Phys. **A405**, 29 (1983).
[10] V. T. Koslowsky, E. Hagberg, J. C. Hardy, G. Savard, H. Schmeing, K. S. Sharma, and X. J. Sun, Nucl. Instrum. Methods Phys. Res. A **401**, 289 (1997).
[11] P. M. Endt, Nucl. Phys. **A521**, 1 (1990).
[12] G. Azuelos, J. E. Kitching, and K. Ramavataram, Phys. Rev. C **15**, 1847 (1977).
[13] G. L. Wick, D. C. Robinson, and J. M. Freeman, Nucl. Phys. **A138**, 209 (1969).
[14] E.-A. McGonigle, J. J. Liggat, R. A. Pethrick, S. D. Jenkins, J. H. Daly, and D. Hayward, Polymer **42**, 2413 (2001).
[15] Handbook of Chemistry and Physics, 77th ed., 1996–1997, edited by D. R. Lide (Editor in Chief).
[16] J. S. Ryder, G. J. Clark, J. E. Draper, J. M. Freeman, W. E. Burcham, and G. T. A. Squier, Phys. Lett. **B43**, 30 (1973).
[17] D. H. Wilkinson and D. E. Alburger, Phys. Rev. C **13**, 2517 (1976).